

Sunil Kumar Meluru Ramesha - Eva Schmidova

STRENGTH AND FRACTURE BEHAVIOUR OF DUAL PHASE STEEL DP450 IN STATIC AND DYNAMIC CONDITIONS

In this work, strength and plastic deformation effect of the dual phase steel are analysed in the static and dynamic conditions. Since the dual phase steel is extensively used in the outer body parts of the automotive vehicles, its dynamic strength and plastic strain energy absorption during the crash are essential. Dynamic strength of the dual phase steel is examined using the pendulum impact hammer tester machine. Spread of the plastic strain during the crash is an important factor for the energy absorption to passive safety, which is examined using the local hardness measurement using the Vickers hardness and local indentation yield strength is calculated using cylindrical indenter and obtained force-depth results are analysed using the Hencky theory for the plane strain indentation. Further, tested samples are observed using scanning electron microscopy for the fracture response after the static and dynamic tests.

Keywords: dual phase steel, plastic deformation, indentation, fracture response and Hencky theory

1 Introduction

Increased demand for fuel efficiency and environmental concern forced the automotive industry to reduce the gross weight of a vehicle. This factor forced the steel manufacturing industry to develop new high strength steel, which has higher strength and lower weight compared to normal steel. Different types of high strength steels are being used in the automotive industry for several decades especially in outer body components. The usage of the dual phase steel in the outer body parts is constantly increasing. In this work, the HCT 450X ferritic-martensitic dual phase steel is used for analysis of strength and plastic deformation ability in static and dynamic conditions. Along with the ferritic-martensitic structure, it has manganese to increase the strength and stabilize the austenite, silicon to enhance the ferrite transformation. The dual phase steel examined here is extensively used in the outer body parts of the automotive applications. Since the outer body parts are exposed to the environment and first form of resistance during the crash and minor accidents, these steels are required to have good corrosion resistance ability, high strength to weight ratio, better weldability, high formability and high strain energy. The higher strain energy is one of the important factors to be considered during the passive safety of automobiles. Presence of higher martensite content increases the strength of the DP steel but further increase in the content of martensite reduces the formability [1-3].

Huang et al. [4] have examined the dual phase strain hardening behaviour and their grain structure changes. Ghassemi-Armaki et al. [5] have worked on the deformation behaviour of martensite and ferrite in the dual phase steel.

In this work, static and dynamic strengths, as well as the plastic strain spread of the dual phase steel are examined.

The strength of the dual phase steel is examined in static and dynamic conditions using the universal tensile testing machine and dynamic pendulum impact tester machines. The spread of the plastic deformation is the key factor in determining the strain energy absorption during the crash, which is analysed by measuring the hardness and micro-indentation yield strength after the testing of samples. Variation of the local hardness and local indentation yield strength are the important parameters to analyse the spread of the plastic strain after the static and dynamic tests. Local hardness is measured using Vickers indenter and local indentation yield strength is measured using the cylindrical indenter and evaluated from the Hencky theory for plane strain indentation.

2 Materials and methods

Table 1 shows the chemical composition of the examined dual phase steel HCT 450X and Figure 1 shows the SEM image with artificial colour of the dual phase steel having ferritic-martensitic phases. Yellow colour phase is the martensitic phase and black colour phase is ferrite.

2.1 The dual phase steel strength in the static and dynamic conditions

To find out the strength of the dual phase steel in the static condition, the standard static tensile test has been performed using the Zwick universal tensile testing machine. The force-displacement graph yield strength and ultimate tensile strength are recorded in computers.

Sunil Kumar Meluru Ramesha*, Eva Schmidova

Faculty of Transport Engineering, University of Pardubice, Czech Republic

*E-mail of corresponding author: Sunilmr21@gmail.com



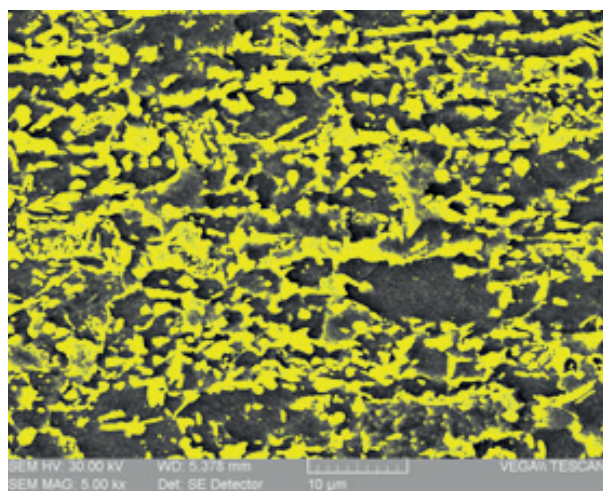


Figure 1 Dual phase steel SEM image

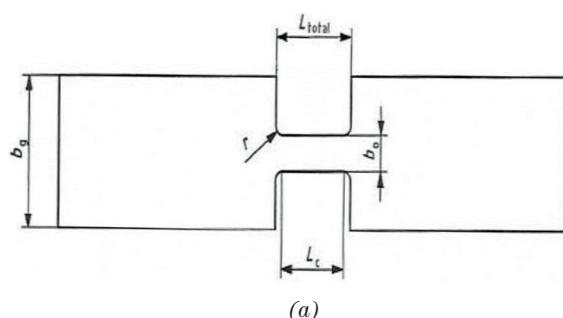
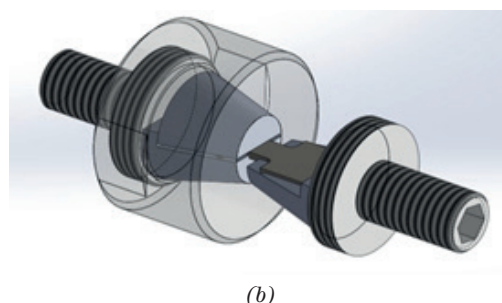


Figure 2 (a) Test specimen for the dynamic impact test and (b) special holder



The dynamic strength test of the dual phase steel is performed in the Zwick pendulum impact hammer tester. The specimen dimensions are $b_g = 15$ mm, $b_0 = 5$ mm, $L_{total} = 9$ mm, $L_c = 5$ mm, $r = 2$ mm. The used samples including holder are presented in Figures 2(a) and 2(b), respectively. A special type of holder is designed in the laboratory to perform the impact test for the dual phase steel in the pendulum impact tester.

2.2 Hardness measurement and fracture behavior of the dual phase steel

Energy absorption during the collision is the key factor. The strain energy absorption during the collision is dependent on the plastic deformation and strain hardening ability of the material. To approximate the residual hardening and spread of the plastic deformation after the static test, the Zwick hardness testing machine is used. After the tensile test, the specimen is cut in the longitudinal direction then grinded and polished. The hardness of the sample is measured from the fractured end to the unaffected end, using the Vickers method. To see the fracture response in the sample after the static and dynamic tests, images are taken in the optical and electron microscope at different magnifications to analyze the fracture type and microscopic fracture behaviour.

Table 1 Chemical composition of the dual phase steel

| Element | Weight percentage |
|---------|-------------------|
| C | 0.130 |
| Mn | 1.933 |
| Si | 0.200 |
| P | 0.022 |
| S | 0.002 |
| Cr | 0.187 |
| Ni | 0.018 |
| Cu | 0.017 |
| Ti | 0.026 |
| Al | 0.022 |

2.3 The yield strength using macro-indentation

While the hardness as a material parameter can be employed as comparative information of UTS, it doesn't reflect the complex transition micro versus macro-plasticity in steel. A complex elastic-plastic response, as comprehensive information about the material response to loading, is required for the real interpretation of the process, which took place during the static versus dynamic loading. The local yield strength must be evaluated in tight connection with microstructure characterization of the loading volume of steel.

To find out the better distribution of plastic deformation and residual hardening effect of the fracture, the macro-indentation technique is used to determine the local yield strength with 0.5 mm diameter cylindrical indenter. Based on the elastic-plastic transition of the curve in the force-depth graph, the yield strength is calculated [6].

The indentation force level at the transition from elastic to plastic state is calculated using the simple curve deviation technique. The Hencky theory for plane strain indentation slip is used to calculate the real yield strength. The ratio of indentation yield strength to normal yield strength is 2.57 according to Hencky equations for the plane strain indentation [7-8]. Pressure relative to the shear yield strength is $P_{indent}/2k=2.57$. Calibration was performed to get precise results for tested steel by the standard tensile test of uninfluenced steel. Figure 3 shows the calculation

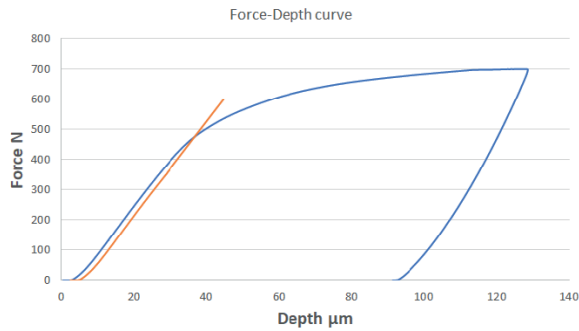


Figure 3 Force-depth curve from indentation test

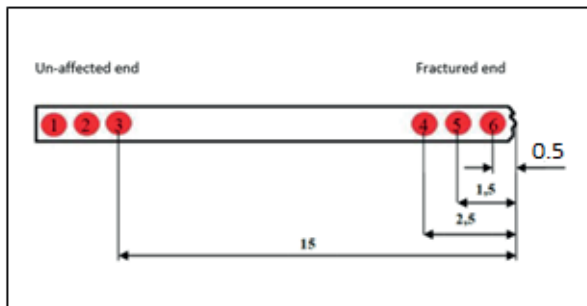


Figure 4 Yield strength measurement positions using indentation technique [9]

of elastic-plastic transition force using the force-depth indentation curve.

Figure 4 shows the indentation yield strength measurement of the dual phase steel sample after the static tensile or dynamic impact test. Three indentation readings are measured close to the fractured end with a gap of 1 mm each. Another three hardness measurements are made at the unaffected end to have a better comparison of hardness values.

3 Results and discussions

3.1 Strength of the dual phase steel

Figure 5 shows the static test results of the dual phase steel performed using the universal tensile testing machine. The average yield strength of the dual phase steel is about 670 MPa and the average ultimate tensile stress is about 770 MPa. The values clearly indicate the higher strength of the dual phase steel compared to interstitial free steel, bake hardened and the high strength steel but still lower than TWIN and advanced high strength steel.

Figure 6 shows the dynamic impact test results of the dual phase steel performed using the pendulum hammer impact tester. The average ultimate tensile strength in dynamic conditions is about 1100 MPa. Values of the UTS in the dynamic conditions are considerably higher than in the static conditions. A special type of holder is designed for the smaller sample size and to reduce the vibrations. The vibrations' effect of the dynamic impact test is eliminated using the polynomial equations of the higher order and the

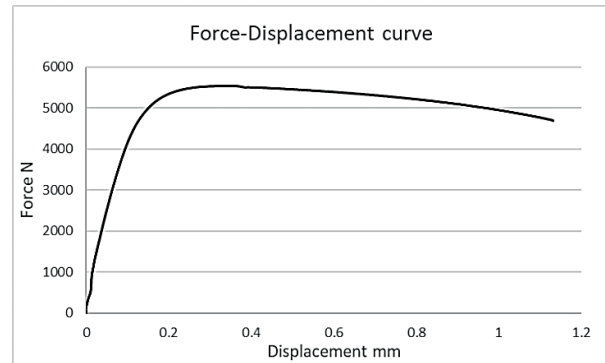


Figure 5 Force-displacement graph for the static tensile test

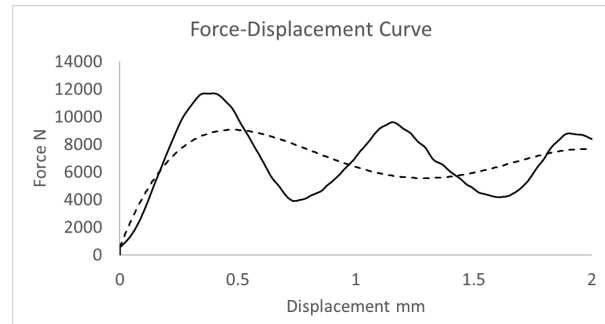


Figure 6 Dynamic test results from impact pendulum tester

sample having the minimum of three waves are selected based on the literature review.

3.2 Fracture response of the DP steel in static and dynamic conditions

Figure 7 shows the SEM image of the fractured surface of dual phase steel after the static tensile test. Fractured surface clearly indicates the ductile fracture mode with the coalescence of micro voids.

Figure 8 shows the SEM image of the fractured surface of the dual phase steel after the dynamic impact test. A clear ductile fracture can be seen even after the impact test with the presence of the transverse cracks. It has pointed to the increased sensitivity of the steel to internal imperfections. Important results towards the current application are the fact that even at the maximal tested strain rate of 1060 /s, the ductile mechanism was retained. The real states of metallurgy quality did not lead to transition to the brittle fracture mode. The critical issue from this point of view can be the presence of brittle, sharp secondary phases and imperfections, e.g. carbonitrides, complex oxides. Sulfides are not commonly critical, except for the case intensive plastic deformation. All observed critical parts were checked and based on that it can be stated that the tested steel has no tendency to transition fracture behaviour inside the analyzed range of strain rate. The energy consumption is driven much more by the spread of plasticity, restricted according to the dynamic loading conditions.

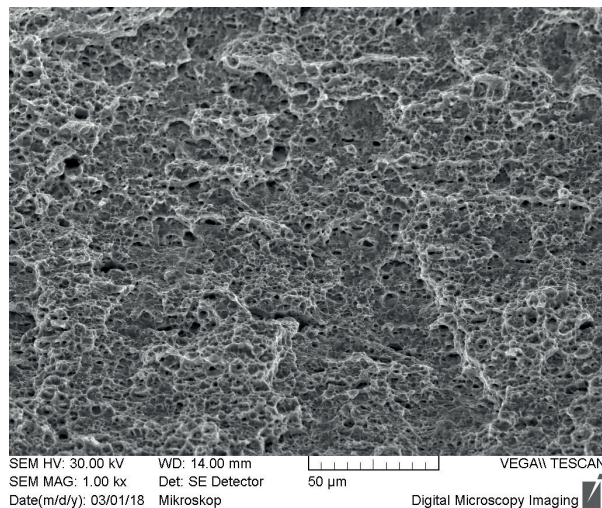


Figure 7 The SEM image of the fractured surface after the static test

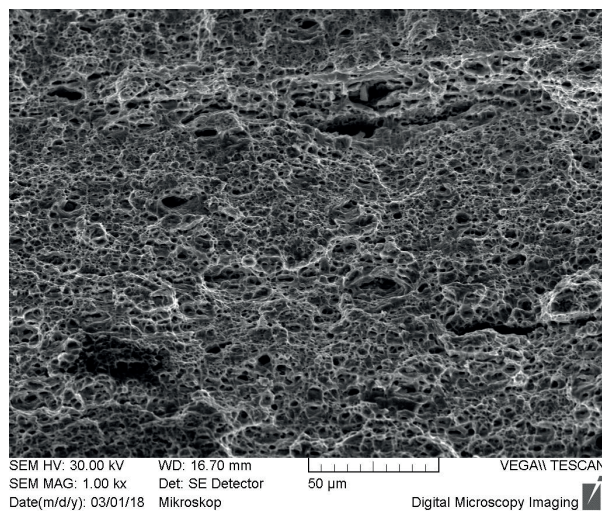


Figure 8 The SEM image of the fractured surface after the dynamic test

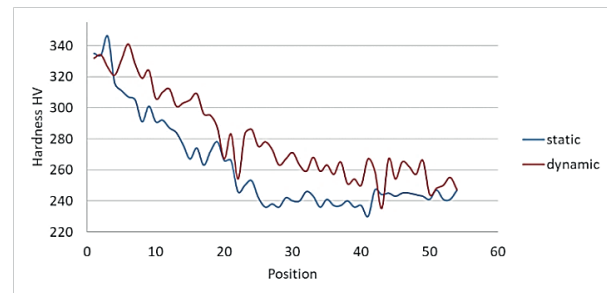


Figure 9 Hardness distribution from fractured end to unaffected end

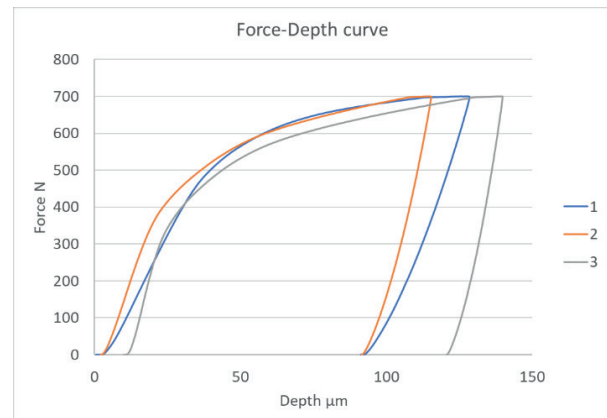


Figure 10 The force-depth curve for the static sample from the fractured end

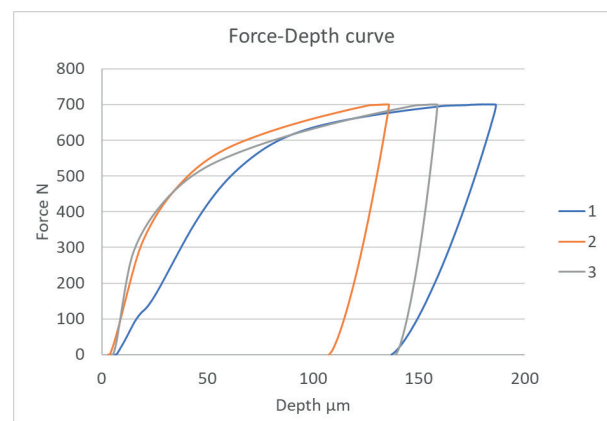


Figure 11 Force -Depth curve for the dynamic sample from the fractured end

3.3 Hardness values

Figure 9 shows the hardness values measured in hardness testing machine using the Vickers indenter. The graph is constructed based on the hardness values from fractured end to the unaffected end for both static and dynamic samples. The high hardness values are being recorded near the fractured end and decrease as it moves towards the unaffected end. Plastic deformation is not the same for the static and dynamic conditions, which can be identified using the hardness values. In the case of the static sample, the spread of the plastic deformation is large and comparatively low hardness values are recorded.

The reasons for the large plastic deformation in static conditions are the availability of sufficient time and low strain rate during the static tensile test.

In the case of dynamic samples, the spread of the plastic deformation is limited only close to the fractured end and large portion of the sample is unaffected by the plastic deformation, which is concluded by the slow gradual decrease in the hardness values just after the one or two measurements.

Though the relation between hardness and residual strain is slightly complicated by the fact that hardness increases with the increase of the residual strain [10-11],

Table 2 Local indentation yield strength for static and dynamic samples

| Position | 1 | 2 | 3 | Unaffected area Avg. |
|----------|--------|--------|--------|----------------------|
| Static | 891.98 | 634.30 | 505.46 | 614.48 |
| Dynamic | 832.52 | 675.92 | 595.56 | 614.48 |

hardness is still a suitable measure of the local residual strain distribution.

3.4 Macro-indentation results for the local yield strength

The force-depth graph of the unaffected area is obtained from the indentation using the 0.5 mm cylindrical indenter for the static sample. From the force-depth graph, the transition of the curve from elastic to plastic region is almost identical and follows the same pattern. The average value of force from elastic to plastic deviation is about 310 N. Figure 10 shows the force-depth graph near the fractured end obtained from the indentation test using the 0.5 mm cylindrical indenter. From the force-depth graph it clear that the transition from elastic to plastic behaviour is not the same for all the curves. The reason for the different curve response is attributed to the varying plastic deformation during the static tensile test. The values of force from elastic to plastic deformation are about 450 N, 320 N and 255 N, respectively from the fractured end. Using the Hencky theory for the plane strain indentation slips it is possible to calculate the approximate yield strength of the sample. Values of the yield strength are shown in Table 2 [12-14].

Figure 11 shows the force-depth graph near the fractured end obtained from the indentation test after dynamic impact test. Comparison to results of the static sample, these dynamic sample results are considerably different. Force values from elastic to plastic transition are 420 N, 341 N and 300 N, respectively. The sudden drop of the elastic-plastic transition force value from 420 N to 341 N indicates the shorter spread of the plastic deformation during the dynamic impact test. The local yield strength is calculated using the Hencky theory for the plane strain indentation and shown in Table 2. Determination of local yield strength is helpful in further confirmation of the area of plastic strain after the static and dynamic tests. Higher yield strength near the fractured area indicates the higher strain hardening effect. Just like hardness, the yield strength is the indicative parameter for the spread of plastic strain, as well.

As stated above, the obtained results have shown the significant influence of strain rate on the capability of tested steel to spread the plasticity. The mentioned process has a crucial effect on energy consumption. The strengthening process, together with the residual stress level is substantially influenced by the local stress-strain

state. This means, that in all the outcomes, the material versus sample dimensions influence should be distinguished. Due to that, the performed analyses must be considered as comparative. Obtained data about the spread of plasticity presents useful information about the influence of the real sample shape and dimensions. Even though in full accordance with valid standards, there is some plastic flow outside the measured area. In the case of restricted part for testing the mentioned effect is not negligible.

4 Conclusion

Comparative analyses of the dual phase steel after loading in static and dynamic conditions were performed. Standard hardness measurement, followed by the indentation tests and evaluation through the Hencky plane strain theory, showed significant sensitivity to strain rate. Observation of the fractured sample in the Scanning Electron Microscopy for the type of fracture response proved the stable fracture mode. Following conclusions are made based on the above observation:

1. The dynamic strengthening of the experimental dual phase steel at an average strain rate 1060s^{-1} is about 43% higher than in the static conditions.
2. Spread of the plastic deformation is considerably different in static and dynamic conditions, large plastic strain spread can be observed in the static test.
3. The spread of the plastic deformation is also confirmed using the Vickers hardness and shows a high value near the fractured end, decreasing gradually towards the unaffected end.
4. Both in the static and dynamic fracture, the mode of fracture are ductile. Which means even at higher loading the material has maintained the ductile fracture mode.
5. The local indentation yield strength helps in further identifying the spread of the plastic deformation and values show the difference in the hardening effect. An optimized methodology using different positioning of the measured points is necessary for a detailed evaluation of discussed processes by used methodology.

Acknowledgement

This study has been accomplished by support of the Grant No: SGS-2018-023.

Reference

- [1] MAZINANI, M. *Deformation and fracture behaviour of a low-carbon dual-phase steel* [online]. Doctoral dissertation. Vancouver: University of British Columbia, 2006. Available from: <https://doi.org/10.14288/1.0302172>
- [2] HWANG, B.-C., CAO, T.-Y., SHIN, S. Y., KIM, S.-H., LEE, S.-H., KIM, S.-J. Effects of ferrite grain size and martensite volume fraction on dynamic deformation behaviour of 0.15C-2.0Mn-0.2Si dual phase steels. *Materials Science and Technology* [online]. 2005, **21**(8), p. 967-975. ISSN 0267-0836. Available from: <https://doi.org/10.1179/174328405X47609>
- [3] BEYNON, N. D., OLIVER, S., JONES, T. B., FOURLARIS, G. Tensile and work hardening properties of low carbon dual phase strip steels at high strain rates. *Materials Science and Technology* [online]. 2005, **21**(7), p. 771-778. ISSN 0267-0836. Available from: <https://doi.org/10.1179/174328405X41038>
- [4] HUANG, T. T., GOU, R. B., DAN, W. J., ZHANG, W. G. Train-hardening behaviours of dual phase steels with microstructure features. *Materials Science and Engineering* [online]. 2016, **672**, p. 88-97. ISSN 0921-5093. Available from: <https://doi.org/10.1016/j.msea.2016.06.066>
- [5] GHASSEMI-ARMAKI, H., MAAß, R., BHAT, S. P., SRIRAM, S., GREER, J. R., KUMARA, K. S. Deformation response of ferrite and martensite in a dual-phase steel. *Acta Materialia* [online]. 2014, **62**, p. 197-211. ISSN 1359-6454. Available from: <https://doi.org/10.1016/j.actamat.2013.10.001>
- [6] HANUS, P., SCHMIDOVA, E., SCHMID, M. The possibilities of evaluating the yield strength in the heat affected zones of a weld through indentation. *Defect and Diffusion Forum* [online]. 2015, **368**, p. 20-24. ISSN 1662-9507. Available from: <https://doi.org/10.4028/www.scientific.net/DDF.368.20>
- [7] OLIVER, W. C., PHARR, G. M. An improved technique for determining hardness and elastic modulus using load and displacement sensing indentation experiments. *Journal of material research*. Volume 7, Issue 6 June 1992, p 1564-1583. 1992. [accessed 2018-12-12]. Available from: <https://doi.org/10.1557/JMR.1992.1564>
- [8] BOWMAN, K. *Mechanical behaviour of materials*. New Jersey, USA: John Wiley and sons., 2004. ISBN 978-0471241980.
- [9] ONDRACEK, P. *Study of dynamic strength of dual phase steel for car body*. Diploma thesis. Pardubice: University of Pardubice, Jan Perner Transport Faculty, 2018.
- [10] TOSHA, K. Influence of residual stresses on the hardness number in the affected layer produced by shot peening. 2nd Asia-Pacific Forum on Precision Surface Finishing and Deburring Technology : proceedings [online]. 2002, p. 48-54. Available from: <https://www.shotpeener.com/library/pdf/2005015.pdf>
- [11] ZHANG, P., LI, S. X., ZHANG, Z. F. General relationship between strength and hardness. *Materials Science and Engineering* [online]. 2011, **529**, p. 62-73. ISSN 0921-5093. Available from: <https://doi.org/10.1016/j.msea.2011.08.061>
- [12] LUO, J., LIN, J. A study on the determination of plastic properties of metals by instrumented indentation using two sharp indenters. *International Journal of Solids and Structures* [online]. 2007, **44**(18-19), p. 5803-5817. ISSN 0020-7683. Available from: <https://doi.org/10.1016/j.ijssolstr.2007.01.029>
- [13] LUO, J., LIN, J., DEAN, T. A. A study on the determination of mechanical properties of a power law material by its indentation force-depth curve. *Philosophical magazine* [online]. 2006, **86**(19), p. 2881-2905. ISSN 1478-6435, eISSN 1478-6443. Available from: <https://doi.org/10.1080/14786430600640528>
- [14] ENNIS, B. L., BOS, C., AARNTS, M. P., LEEB, P. D., JIMENEZ-MELERO, E. Work hardening behaviour in banded dual phase steel structures with improved formability. *Materials Science and Engineering A* [online]. 2018, **713**, p. 278-286. ISSN 0921-5093. Available from: <https://doi.org/10.1016/j.msea.2017.12.078>